

A simple model for cavity-enhanced laser-driven ion acceleration from thin foil targets

P. Rączka^{a,*}, J. Badziak^a

^a*Institute of Plasma Physics and Laser Microfusion, 23 Hery Str., 01-497 Warsaw, Poland*

Abstract

A scenario for laser-driven ion acceleration from a thin solid target is considered, where the reflected laser pulse is redirected towards the target by reflection at the inner cavity wall. This scenario is discussed in the context of sub-wavelength foil acceleration in the radiation pressure regime, when plasma dynamics is known to be reasonably well described by the laser-sail model. A semi-analytic extension of the 1D laser-sail model is constructed for this case. The effect of cavity reflections on sub-wavelength foil acceleration is then illustrated with two concrete examples of intense laser pulses of picosecond and femtosecond duration.

Keywords: laser-driven ion acceleration, radiation pressure acceleration,, laser-sail model

PACS: 52.38.Kd, 41.75.Jv

1. Introduction

In the last decade there has been growing interest in laser-driven ion acceleration, where energetic ions are generated by irradiating a thin foil (with thickness in the micrometer range) with an ultra-intense (above 10^{18} W/cm²) laser beam. The laser-generated proton pulses had been used for example for ultra-fast radiography and radioisotope production, and together with laser-generated beams of heavier ions they are of high interest from the point of hadron tumor therapy and fast ignition of inertial confinement fusion targets [1, 2, 3, 4]. The use of an ultra-intense laser as an ion driver offers certain advantages over conventional linear or circular accelerators, allowing for construction of very compact devices that produce particle pulses of high intensity and very short duration. Unfortunately, ion energies achieved so far in this approach are not very high (below 100 MeV per nucleon), and the achieved values of the laser-to-ion energy conversion efficiency are generally below 10% [5, 6].

*Corresponding author

Email address: piotr.raczka@ifpilm.pl (P. Rączka)

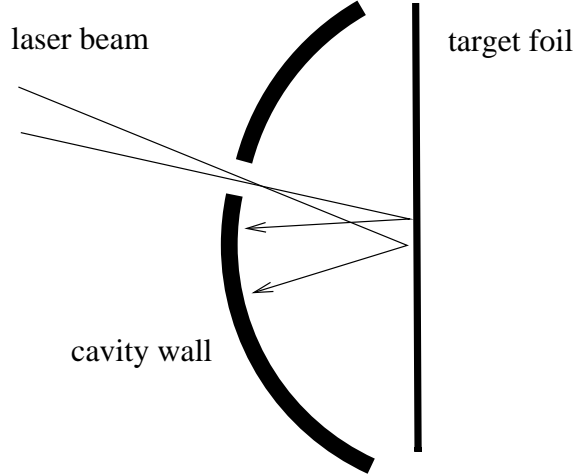


Figure 1: Schematic drawing of a target with the cavity that redirects the reflected pulse towards the foil.

It was recently observed that basic parameters of the accelerated ion pulses - the maximum ion energy, the average ion energy, and the laser-to-ion energy conversion efficiency - could be considerably improved if the target foil is enclosed in a cavity that redirects the laser pulse reflected from the foil back into the foil, thus in a sense “recycling” the laser energy [7, 8]. The mechanism of cavity-enhanced plasma acceleration, dubbed the Laser Induced Cavity Pressure Acceleration (LICPA) mechanism [8, 9], was found to be very effective at sub-relativistic laser intensities ($\sim 10^{15}$ W/cm²), where enhancement in ion acceleration is predominantly due to the buildup of thermal plasma pressure inside the cavity [8, 9, 10]. Computer simulations performed at higher laser intensities, when the radiation pressure becomes important, show that the LICPA mechanism would be effective in this regime as well [7, 8]. A possible target arrangement realizing the LICPA principle in the radiation pressure regime is shown in Fig. 1. A detailed account of these simulations would be reported elsewhere. In this note we discuss a realization of the LICPA idea in the radiation pressure regime, but in a narrower context, namely when plasma dynamics is reasonably well described by the laser-sail (LS) model [11, 12, 13]. Such a situation occurs for example when a high intensity and high contrast laser pulse is incident on a foil of sub-wavelength thickness. This acceleration regime attracted recently considerable attention [14, 15, 16, 17, 18, 19, 20, 21]. We limit our considerations to a one-dimensional approximation and we construct cavity-enhanced LS model, in which the effect of reflections of the laser pulse at the inner cavity wall is taken into account in a semi-analytic way. We illustrate the characteristic features of this implementation of LICPA with concrete predictions for ions generated using a realistic ultra-thin foil target and the laser parameters close to the expected capabilities of the big new laser facilities ELI

[22] and PETAL [23] that would become available in the near future.

2. The laser-sail model in one dimension

Let us consider a thin planar foil of areal mass density σ , irradiated at a normal incidence by an intense laser beam propagating along the x axis. The intensity of the laser beam at the origin of the laboratory reference frame has the temporal profile $I(t)$. Under certain circumstances - for example when the foil has sub-wavelength thickness and the laser pulse is of sufficiently high intensity and high contrast - the overall motion of the accelerated plasma is similar to that of a “sail” driven by the radiation pressure of the laser beam [13]. Furthermore, if the foil thickness exceeds certain minimal value, it acts as a nearly totally reflecting mirror. The equation of motion for such a mirror driven by the laser beam had been first derived in the context of laser-driven interstellar space travel [11, 12]:

$$\frac{d}{dt}(\beta\gamma) = \frac{2I(t - x/c)}{\sigma c^2} R(\omega') \frac{1 - \beta}{1 + \beta}, \quad (1)$$

where $\beta = \frac{1}{c} \frac{dx}{dt}$, $\gamma = 1/\sqrt{1 - \beta^2}$, $\omega' = \omega \sqrt{(1 - \beta)/(1 + \beta)}$ is the laser frequency in the foil rest frame, and $R(\omega')$ denotes the foil reflectivity in its rest frame. We shall further assume $R(\omega') = 1$. This equation may be recast in a particularly useful form by introducing a relativistic retarded time variable $w = ct - x$ [12]:

$$\frac{\gamma}{1 - \beta} \frac{d\beta}{dw} = \frac{2I(w/c)}{\sigma c^3}. \quad (2)$$

By a straightforward integration it is then found that the speed of the foil which was at rest at $w = 0$ is given by [12]

$$\beta(w) = \frac{(1 + e(w))^2 - 1}{(1 + e(w))^2 + 1}, \quad (3)$$

where $e(w)$ is the total laser energy per unit area incident on the foil up to the retarded time w , normalized to the half of the relativistic rest energy per unit area of the foil:

$$e(w) = \frac{2}{\sigma c^3} \int_0^w I(w'/c) dw'. \quad (4)$$

Using the fact that $dx/dw = \beta/(1 - \beta)$ one may obtain the position of the foil as a function of the retarded time w :

$$x(w) = x(0) + \int_0^w \frac{\beta(w')}{1 - \beta(w')} dw'. \quad (5)$$

Taking into account that $ct(w) = w + x(w)$ we obtain this way a complete parametric description for the world line of the foil in the (ct, x) plane in a parametric form. The relativistic kinetic energy of the ions in the foil is found to be

$$E_i(w) = m_i c^2 \frac{e^2(w)}{2[1 + e(w)]} . \quad (6)$$

This very simple 1D model was found to be surprisingly useful in interpreting results of 3D and 2D kinetic simulations for laser ion acceleration. In the case of sub-wavelength foils driven by linearly polarized beams, the laser sail behaviour was famously identified in a 3D simulation at the laser intensity of $1.4 \times 10^{23} \text{ W/cm}^2$ [13]. It was found that the initially planar foil is deformed into a “cocoon”, in which the laser pulse is confined, and a stable plasma clump is formed from the portion of the foil of the size of the pulse focal spot, being then pushed forward by the radiation pressure. (In fact the LS model was used in that paper to extrapolate the ion acceleration beyond the simulation time, which was limited due to insufficient computer resources.) It was later observed that circularly polarized beams create more favorable conditions for such a block acceleration of plasma [24], and a parametric study had shown that the LS-type of behavior becomes visible in 1D simulations for ultra-thin targets already at $I \cdot (\lambda/1\mu\text{m})^2 = 2.8 \times 10^{20} \text{ W/cm}^2$ [20]. The case of linear polarization is more complex, because generally at less extreme intensities a broad energy spectrum is obtained. The most we can hope for is a quasi-monoenergetic peak on a broad background, which becomes clearly visible at the intensity of $5 \times 10^{21} \text{ W/cm}^2$ [25, 26]. It seems then reasonable to expect that evolution of ions in the quasi-monoenergetic peak would be consistent with the LS model. It is interesting to note that the evolution of plasma clumps follows the LS dynamics even though they are not accelerated as rigid bodies and undergo some internal evolution. It is also interesting that the evolution of targets which are relatively thick compared to the laser wavelength is also found to be consistent with the LS dynamics [27, 28]. A generalization of the relativistic LS foil dynamics beyond 1D was outlined in [14, 18] and applied to the study of instabilities in the ultra-thin foil acceleration process.

3. Cavity-enhanced laser-sail model

Let us now consider a generalization of the 1D laser-sail equation to include a contribution from the laser pulse reflected from the target and redirected onto the target through a reflection from the inner wall of the cavity surrounding the target. The enhanced accelerating effect of the laser pulse reflected from the target foil and then redirected towards the target was considered already in [12] in the context of an interstellar space travel driven by an Earth-based laser, but for the laser ion acceleration a more general formula is needed, valid also in the case of an overlap between the original pulse and the pulse reflected at the inner cavity wall.

Let us assume that the laser pulse enters the cavity at $x = 0$ and is totally reflected by the foil located at $x(w)$ (this implies that the foil thickness - being sub-wavelength - has to be larger than certain minimal value). The pulse returns to the inner cavity wall located at $x = 0$ and is then redirected towards the foil

(this is of course an approximation, in a real 3D geometry the reflection at the inner cavity wall would have to occur in a different place than the entrance to the cavity). The distance between the cavity entrance at $x = 0$ and the initial position of the foil $x(0)$ is equal to the cavity depth L_c . Let us denote by w_j , $j = 0, 1, 2, \dots$, the values of the retarded time for which the leading edge of the laser pulse is sent toward the foil from the position of the inner cavity wall for the j -th time. Assuming that the laser pulse begins at $w_0 = 0$, we obviously have $w_1 = 2L_c$. Next, let $x^{(j)}(w)$ denote (for $j \geq 1$) the position of the foil for w in the interval $[w_{j-1}, w_j]$. These functions satisfy an obvious continuity relation $x^{(j+1)}(w_j) = x^{(j)}(w_j)$. Knowing w_j and $x^{(j)}(w_j)$, we obtain w_{j+1} from the formula

$$w_{j+1} = w_j + 2x^{(j)}(w_j). \quad (7)$$

Finally, let $e^{(j)}(w)$ denote (for $j \geq 1$) the total laser energy per unit area of the foil - expressed in the units of a half of the relativistic rest energy per unit area of the foil - that was incident on the foil for w in the interval $[w_0, w_j]$, i.e. during the whole acceleration process up to w_j . The value of $e^{(1)}(w)$ is simply given by the formula 4. The values of $e^{(j)}(w)$ for $j \geq 2$ may be determined iteratively. The expression for $e^{(j+1)}(w)$ consists of three terms: the first representing the total laser energy per unit area incident on the foil until $w = w_j$, the second representing the laser energy per unit area coming from the original laser pulse, incident on the foil in the interval $[w_j, w]$, and the third representing the laser energy per unit area that had been reflected from the foil in the interval $[w_{j-1}, w_j]$ and was redirected towards the foil. The laser energy per unit area reflected from the foil in an interval $[w_a, w_b]$ is given by the formula

$$\frac{\sigma c^2}{2} \frac{e(w_b) - e(w_a)}{[1 + e(w_b)][1 + e(w_a)]}, \quad (8)$$

but only a fraction R_c of this is redirected to the foil by the reflection at the inner cavity wall. (For simplicity we shall assume in the following that R_c is constant, whereas in reality it could show some dependence on laser intensity and material properties of the inner cavity wall.) Taking into account all contributions we obtain

$$e^{(j+1)}(w) = e^{(j)}(w_j) + \frac{2}{\sigma c^3} \int_{w_j}^w I(w'/c) dw' + R_c \frac{e^{(j)}(w_{ref}^{(j)}(w)) - e^{(j)}(w_{j-1})}{[1 + e^{(j)}(w_{ref}^{(j)}(w))][1 + e^{(j)}(w_{j-1})]}, \quad (9)$$

where the function $w_{ref}^{(j)}(w)$ is a solution of an implicit equation

$$w = w_{ref}^{(j)} + 2x^{(j)}(w_{ref}^{(j)}), \quad (10)$$

i.e. it represents the value of the retarded time variable from the interval $[w_{j-1}, w_j]$ for which a redirected ray that is incident on the foil at $w \in [w_j, w_{j+1}]$ was for the last time reflected from the foil. Obviously, $w_{ref}^{(j)}(w_j) = w_{j-1}$. The

relativistic speed $\beta^{(j+1)}(w)$ in the interval $w \in [w_j, w_{j+1}]$ is obtained by substituting $e^{(j+1)}(w)$ into the Eq. 3. The position of the foil is then obtained from the formula similar to Eq. 5:

$$x^{(j+1)}(w) = x^{(j)}(w_j) + \int_{w_j}^w \frac{\beta^{(j+1)}(w')}{1 - \beta^{(j+1)}(w')} dw'. \quad (11)$$

The relativistic kinetic energy of the accelerated ions for $w \in [w_0, w_j]$ is given by the formula 6 with $e(w)$ replaced by $e^{(j)}(w)$.

4. Concrete examples

Let us consider the predictions of the cavity-enhanced LS model in two concrete scenarios characterized by the same total laser fluence, but with distinctly different pulse lengths. The first scenario involves a laser pulse with the maximum intensity of 10^{22} W/cm² and the full width at half maximum equal to $t_{HW} = 130$ fs; such parameters should be attainable for example with a slightly defocused kilojoule beam at the future ELI Beamlines facility [22]. The second scenario involves a pulse with the duration of 1.3 ps, i.e. larger by an order magnitude, but with lower maximum intensity, equal to 10^{21} W/cm²; such parameters should be available for example at the future PETAL facility [23]. The temporal profiles of these pulses are taken to be super-Gaussian, and they are assumed to start at the intensity smaller by a factor of 100 relative to the maximum intensity: $I(t) = I_0 \exp[-((t - t_p)/2)/\tau)^6]$ for $t \in [0, t_p]$, where $t_p = t_{HW}(\log 100 / \log 2)^{1/6}$ and $\tau = \frac{1}{2}t_{HW}/(\log 2)^{1/6}$. The laser energy fluence on target in both scenarios is equal to $12.81 \text{ J}/(\mu\text{m})^2$.

Our target is assumed to be an ultra-thin carbon foil, with the density of 2.2 g/cm^3 . For the foil to be nearly completely reflective it cannot be too thin. In 1D the condition for nearly total reflection takes the form [20, 21] $\pi(l/\lambda) \cdot (n_e/n_c) > a_0$, where λ is the laser wavelength (which is either 800 nm for ELI or 1054 nm for an Nd:glass picosecond laser), n_e is the plasma electron density, $n_c = (4\pi^2 c^2 m_e \varepsilon_0 / e^2) \cdot (1/\lambda^2)$ is the critical electron density for a given wavelength (m_e is the electron mass), and a_0 is the dimensionless laser field amplitude, related to the intensity I by the relation $I = \alpha m_e c^3 n_c a_0^2$ ($\alpha = 1$ for circular polarization and $\alpha = 1/2$ for linear polarization). The non-transparency condition may be rewritten in the form

$$l > \frac{2}{en_e} \sqrt{\frac{\varepsilon_0 I}{c\alpha}}. \quad (12)$$

For a fully ionized carbon we have $n_e = 6.62 \cdot 10^{23} \text{ cm}^{-3}$, so for a circularly polarized beam with $I = 10^{22} \text{ W/cm}^2$ we obtain a condition $l > 32 \text{ nm}$. However, to leave some margin for the foil thinning due to the 3D stretching, as well as possible prepulse issues which might be important in the case of kilojoule beams, we assume $l = 200 \text{ nm}$.

As for the cavity parameters, in both cases we choose $L_c = 80 \mu\text{m}$, which seems to be a technologically achievable value. The reflection coefficient at the

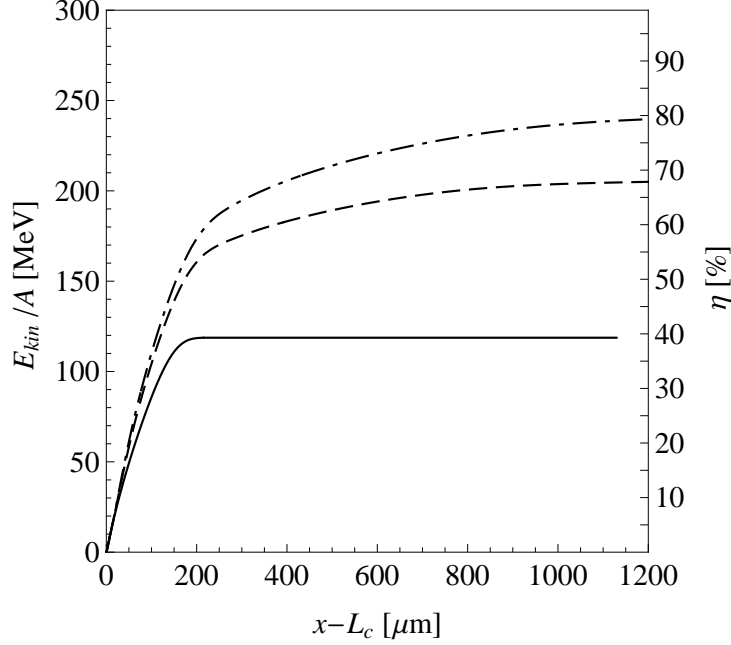


Figure 2: Ion energy per atomic mass unit, as a function of the acceleration distance, for the case of 1.3 ps pulse with 10^{21} W/cm² peak intensity. Solid line indicates acceleration without cavity reflection, while the dash-dotted (dashed) line indicates an acceleration with the fraction $R_c = 0.8$ ($R_c = 0.6$) of the laser energy being reflected at the inner cavity wall.

inner cavity wall R_c is a free parameter in this model. We assume $R_c = 0.8$ and for comparison we give also the results obtained for $R_c = 0.6$; a more precise determination of R_c would require computer modelling of the cavity beyond the 1D approximation.

In Fig. 2 we show the evolution of the ion energy per atomic mass unit of ion mass (i.e. E_{ion}^{kin}/A , where A is the ion mass number) as a function of the acceleration distance for the 1.3 ps pulse with 10^{21} W/cm² peak intensity. The evolution in the absence of the cavity reflections is indicated by the solid line: the foil is rapidly accelerated over a distance of 215 μ m to the energy of 119 MeV/u, and then “sails away” at a constant speed.

If reflections at the inner cavity wall are taken into account with the fraction of $R_c = 0.8$ of the laser energy reflected at the inner cavity wall, the acceleration of the foil is continuously enhanced by the laser pulse redirected multiple time towards the target by reflection at the inner cavity wall (as indicated by the dash-dotted line), which nearly doubles the resulting ion energy relative to the case without the cavity reflection. For $R_c = 0.6$ (dashed line) the energies to which the ions are accelerated are slightly smaller, but the general pattern is the same.

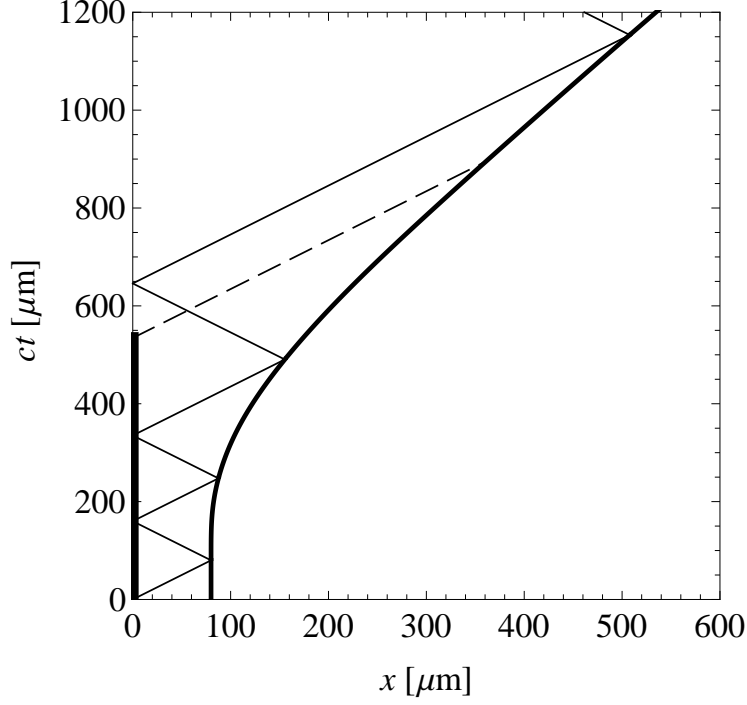


Figure 3: A space-time plot of successive reflections of the incident laser pulse from the accelerated foil and the inner cavity wall for the 1.3 ps pulse with 10^{21} W/cm² peak intensity, with the fraction $R_c = 0.8$ of the laser energy being reflected at the inner cavity wall.

The result for the ion energy per a.m.u. is easily converted into the laser-to-ion conversion efficiency, which is shown on the right side of the figure. The total ion energy per unit surface area of the target is given by $(E_{ion}^{kin}/A) \cdot (\sigma/u)$, where u is the atomic mass unit, so every 10 MeV of ion energy per a.m.u. corresponds to the ion beam energy fluence of 42.45 MJ/cm², which implies a laser-to-ion energy conversion efficiency of 3.31%. Note that the acceleration efficiency is quite high - around 40% - even without the cavity reflections, which is characteristic of the radiation pressure acceleration [13, 20].

A space-time plot of successive reflections of the incident pulse in this case is presented in Fig. 3. The thick segment along the vertical axis indicates duration of the initial pulse at the entrance to the cavity, the moderately thick solid curve indicates the world line of the foil, the thin solid line indicates the world line of the leading edge of the pulse, including the reflections from the accelerated foil and the inner cavity wall, and the dashed line indicates the world line of the trailing edge of the pulse. As we see, there is a substantial overlap between the incident pulse and the reflected pulse in this case.

The evolution of ion energy per a.m.u. for the case of 130 fs pulse with

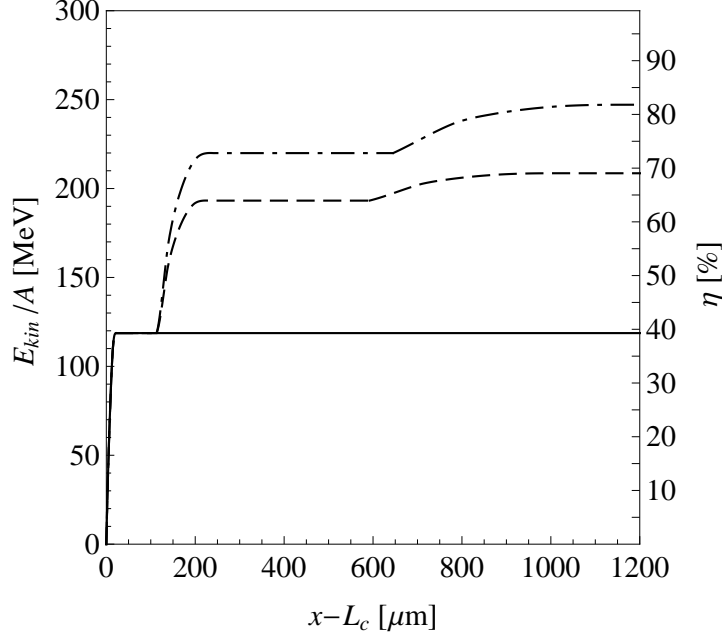


Figure 4: Ion energy per atomic mass unit, as a function of the acceleration distance, for the 130 fs pulse with 10^{22} W/cm 2 peak intensity. Solid line indicates acceleration without cavity reflections, while the dash-dotted (dashed) line indicates the acceleration with the fraction $R_c = 0.8$ ($R_c = 0.6$) of the laser energy being reflected at the inner cavity wall.

10^{22} W/cm 2 peak intensity is shown in Fig. 4. If there are no cavity reflections, the foil is rapidly accelerated over a very short distance of 22 μm , achieving the same energy as in the previous case, and then “sails away” at a constant speed. If reflections at the inner cavity wall are taken into account (with $R_c = 0.8$), the foil receives additional kick by the redirected pulse, which re-interacts with the foil at the distance of 113 μm from its initial position, again nearly doubling the ion energy (and the conversion efficiency as well). After being reflected by the foil for the second time the pulse is redirected onto the foil once again and hits the moving foil for the third time at the distance of 645 μm from its initial position, but the effect of this third impact is rather small. It should be noted that the spatial extent of the femtosecond pulse is small compared to the chosen cavity depth, so the foil flies freely before being hit by the redirected pulse. For $R_c = 0.6$ the energies of the accelerated ions are slightly smaller, but the general pattern is the same.

Interestingly, energies achieved over the acceleration distance of several hundred micrometers in this scenario are very close to energies achieved with the ps pulse, which indicates that higher order reflections have only small effect on the resulting ion energies. This is an important observation from the point of view of designing targets with a cavity, because it shows that it is enough

for the cavity reflector to survive only few reflections, since the loss of further reflections due to a deteriorating cavity wall would not significantly affect the final result.

However, this picture could be different if a more dense target is used, for example a metal foil. Such foil would accelerate less rapidly, so even for a small acceleration distance many cavity reflections could occur. The ion energy per a.m.u. achieved in the pure LS mode would be small in this case, but the enhancement due to presence of the cavity could be much bigger than 100%. The question is whether the foil and the cavity would survive as a solid body after large number of reflections.

Finally, it is an interesting issue how the acceleration energies depend on the depth of the cavity L_c . We studied this issue for the case of the picosecond pulse. Somewhat surprisingly, it was found that the ion energies measured at the acceleration distance of $300\text{ }\mu\text{m}$ show only a mild dependence on the cavity depth: for $L_c = 40, 60, 80, 100, 120, 140\text{ }\mu\text{m}$ the values of ion kinetic energy per a.m.u. were respectively 208, 202, 195, 186, 179, 175 MeV. For the femtosecond pulse the dependence would be even smaller, since even for the smallest of the considered cavities there would be no overlap between the incident pulse and the redirected pulse.

5. Conclusions

Summarizing, we constructed a simple implementation of the LICPA mechanism for laser ion acceleration in the radiation pressure domain, based on a semi-analytic 1D laser-sail model. The model accomodates in a general way the additional contribution from pulses reflected from the target foil and redirected towards the target via reflection at the inner cavity wall. We used this model to obtain concrete predictions for acceleration of an ultra-thin carbon foil, driven by laser pulses of different duration - a fs range pulse and a ps range pulse - and different intensity, but the same laser fluence, providing a convincing illustration of characteristic features of LICPA. The possibility of a considerable increase in the ion energy and the laser-to-ion conversion efficiency, as large as 50% or more, was clearly demonstrated. Our predictions could serve as a guide for experiments at the laser facilities that would become available in the near future. Although in principle the cavity-enhanced LS model is applicable to ultra-thin foil acceleration, it is not unreasonable to expect that it would turn out to be useful in interpreting the results for averaged quantities obtained in numerical simulations and experiments involving thicker targets, as had been indicated in [7, 27, 28].

P. Rączka gratefully acknowledges ESF support in the form of the SILMI RNP grant No. 3638.

References

- [1] G. A. Mourou, T. Tajima, and S.V. Bulanov, Rev. Mod. Phys. 78 (2006) 309.

- [2] M. Borghesi *et al.*, Fusion Science and Technology 49 (2006) 412.
- [3] J. Fuchs *et al.*, Nature Phys. 2 (2006) 48.
- [4] L. Robson *et al.*, Nature Phys. 3 (2007) 58.
- [5] D. Jung *et al.*, Phys. Rev. Lett. 107 (2011) 115002.
- [6] B. M. Hegelich *et al.*, Nuclear Fusion 51 (2011) 083011.
- [7] J. Badziak, S. Jabłoński, and P. Rączka, *Efficient generation of high-energy quasi-monoenergetic ion beams using laser-induced cavity pressure acceleration*, P5.038, 38th EPS Conference on Plasma Physics, 27 June - 1 July 2011, Strasbourg, France.
- [8] J. Badziak *et al.*, Phys. Plasmas 19 (2012) 053105.
- [9] J. Badziak *et al.*, App. Phys. Lett. 96 (2010) 251502.
- [10] S. Borodziuk *et al.*, Appl. Phys. Lett. 95 (2009) 231501.
- [11] G. Marx, Nature 211 (1966) 22.
- [12] J.F.L. Simmons and C. R. McInnes, Am. J. Phys. 61 (1993) 205.
- [13] T. Esirkepov *et al.*, Phys. Rev. Lett. 92 (2004) 175003.
- [14] F. Pegoraro and S. Bulanov, Phys. Rev. Lett. 99 (2007) 065002.
- [15] A. P. L. Robinson *et al.*, New J. Phys. 10 (2008) 013021.
- [16] O. Klimo, J. Psikal, J. Limpouch, and V. T. Tikhonchuk, Phys. Rev. ST-AB 11 (2008) 031301.
- [17] T. V. Liseykina *et al.*, Plasma Phys. Control. Fusion 50 (2008) 124033.
- [18] S. V. Bulanov *et al.*, C. R. Physique 10 (2009) 216.
- [19] B. Qiao, M. Zepf, M. Borghesi, and M. Geissler, Phys. Rev. Lett. 102 (2009) 145002.
- [20] A. Macchi, S. Veghini, and F. Pegoraro, Phys. Rev. Lett. 103 (2009) 085003.
- [21] A. Macchi, S. Veghini, T. V. Liseykina and F. Pegoraro, New J. Phys. 12 (2010) 045013.
- [22] *ELI - Extreme Light Infrastructure Whitebook*, G. Mourou, G. Korn, W. Sandner, J. L. Collier (eds.), Thoss Media, Berlin 2011.
- [23] N. Blanchot *et al.*, Plasma Phys. Control. Fusion 50 (2008) 124045.
- [24] A. Macchi, F. Cattani, T. V. Liseykina, and F. Cornolti, Phys. Rev. Lett. 94 (2005) 165003.

- [25] T. Esirkepov, M. Yamagiwa, and T. Tajima, Phys. Rev. Lett. 96 (2006) 105001.
- [26] A. V. Brantov *et al.*, Nucl. Instrum. Methods Phys. Res. A 653 (2011) 62.
- [27] M. Grech *et al.*, New J. Phys. 13 (2011) 123003.
- [28] J. Badziak and S. Jabłoński, Appl. Phys. Lett. 99 (2011) 071502.